The International Journal of Advanced Manufacturing Technology (2018) 99:225–232
https://doi.org/10.1007/s00170-018-2517-5

ORIGINAL ARTICLE

Simulation tool for prediction of cutting forces and surface quality of micro-milling processes

Klaus Schützer[1] · Luciana Wasnievski da Silva de Luca Ramos[2] · Jan Mewis[3] · Marcelo Octavio Tamborlin[1] · Crhistian Raffaelo Baldo[4]

Received: 26 March 2018 / Accepted: 25 July 2018 / Published online: 1 August 2018

Abstract
The improvement of micro-milling processes implies the application of advanced analysis and modeling techniques to derive a deeper process understanding. Because of micro-scale effects, monitoring, and measurement systems applied in conventional milling are in most cases not suitable for identifying optimal cutting conditions. Therefore, analytical and mechanical models have been developed in recent years to account for impact factors dominating the micro-milling errors. Within the research presented in this publication, geometric, kinematic, and dynamic models have been adjusted and dimensioned according to the dominating impact factors in micro-milling and have been consolidated to enable for a time-domain simulation. The effect of element size of discretized workpiece and tool as well as the time step size on cutting forces has been evaluated. The accuracy of predicting cutting forces has been investigated and a good agreement of measured and simulated cutting forces has been found. Finally, a mold for a micro-fluidic device has been machined virtually and experimentally to evaluate the accuracy of the integrated models in predicting the final quality of a micro-milled part in terms of surface quality parameters.

Keywords Micro-milling · Virtual machining · Cutting forces · Surface quality

1 Introduction

Micro-machining enables the production of miniaturized parts as well as high precision machining of functional surfaces. The micro-milling process behavior is different from macro-cutting. Chip thickness and grain sizes of different materials are in the range of the cutting edge radius dimension. Typical application fields are parts of the optical industry and molds with microstructures [1]. Some critical issues in micro-milling processes regarding the tool performance are related to the size of components, cutting operations, and the tool itself. Compared to macro-milling tools, miniature tools are subject to large deflection and high stress during machining, due to reduced stiffness and size effect.

A micro-device can be defined as having at least two critical dimensions in the sub-millimeter range [2] or a component whose feature has at least one critical dimension significantly smaller than 0.1 mm, typically with tolerance ranges of a few micrometers, while the whole device may have larger dimensions [3]. This typical miniaturized component creates a

✉ Marcelo Octavio Tamborlin
marcelo.tamborlin@scpm.unimep.br

Klaus Schützer
schuetzer@scpm.unimep.br

Luciana Wasnievski da Silva de Luca Ramos
swluciana@ipt.br

Jan Mewis
mewis@iwf.tu-berlin.de

Crhistian Raffaelo Baldo
crhistian.baldo@ufabc.edu.br

[1] Universidade Metodista de Piracicaba - Lab. de Sistemas Computacionais para Projeto e Manufatura, Rod. Luis Ometto (SP 306) Km 24, Santa Barbara d'Oeste 13451-900, Brazil

[2] IPT Instituto de Pesquisas Tecnológicas - Núcleo de Bionanomanufatura, Av. Prof. Almeida Prado, 532, São Paulo 05508-901, Brazil

[3] Technische Universität Berlin - Institut für Werkzeugmaschinen und Fabrikbetrieb, Produktionstechnisches Zentrum (PTZ), Pascalstraße 8 - 9, 10587 Berlin, Germany

[4] Universidade Federal do ABC - Centro de Engenharia, Modelagem e Ciencias Sociais Aplicadas, Avenida dos Estados, 5001, Santo André, SP 09210-580, Brazil

multi-fold measurement problem [3, 4]. The smaller the absolute scale, the more challenging is the measurement task due to the required environment control. Aspect ratio of critical features imposes additional constraints regarding probe size and feature accessibility. The complexity increases in the determination of the associated measurement uncertainties, and in the validation of measurement procedures to ensure the requested confidence on results [5].

The efficient improvement of micro-milling processes implies the application of advanced analysis and modeling techniques. Because of scaling effects, monitoring and measurement systems applied in conventional milling are in most cases not suitable for identifying optimal cutting conditions for micro-milling processes. Therefore, analytical and mechanistic models have been developed in recent years to account for impact factors dominating the micro-milling errors, which usually imply the modeling of cutting forces. They consider chip thickness and formation, cutting edge radius, process damping, and the compliance at the tool center point (TCP), which has been investigated by many researchers [6–10]. Nowadays, virtual machining systems are appropriate tools to estimate the process safety, the machining accuracy, and part quality, and therefore, also to derive improvements by software-in-the-loop optimization [11].

This publication describes the development of a time-domain simulation tool to predict surface quality and cutting forces of micro-milling process. To achieve this goal, geometric, kinematic, and dynamic models have been adjusted and dimensioned according to the dominating impact factors in micro-milling and have been consolidated in a simple GUI application.

2 Experiments

Cutting experiments have been conducted on the ultra-precision machining center KERN Evo, KERN Microtechnik GmbH. The manufacturing process realization is illustrated in Fig. 1. First, a cutting parameter study was established aiming at detecting and analyzing the impact of cutting parameter on surface roughness and cutting forces. In a consecutive step, an exemplary micro-mold was machined using the parameter set with an adequate surface roughness to productivity ratio. The CAD/CAM program Siemens NX 10, Siemens PLM Software, has been used to design the workpiece and generate the tool paths.

Tool diameter and length have been measured using the inbuilt tool setter P87.0634-015-NT/laser control nano NT, Blum-Novotest GmbH. The workpiece referencing has been done by scratching in z-direction while monitoring the contact area with a high sensitivity CCD camera WAT-231S2, WATEC CO., to obtain the first contact. The machine tool has been in a warmed-up state. Referencing in x- and y-direction has been conducted using a wireless 3D touch probe, Infrared Probe 32.00-MINI HDR, M&H Inprocess Messtechnik GmbH. For the machining, rough, semi-finishing, and finishing process have been done using solid carbide end-mills with diameter $d = 8$, 4, 2, 1, and 0.4 mm from Arno tools, Karl-Heinz Arnold GmbH. In addition, the positioning error of the machining center has been determined using a XL-80 laser interferometer, Renishaw plc.

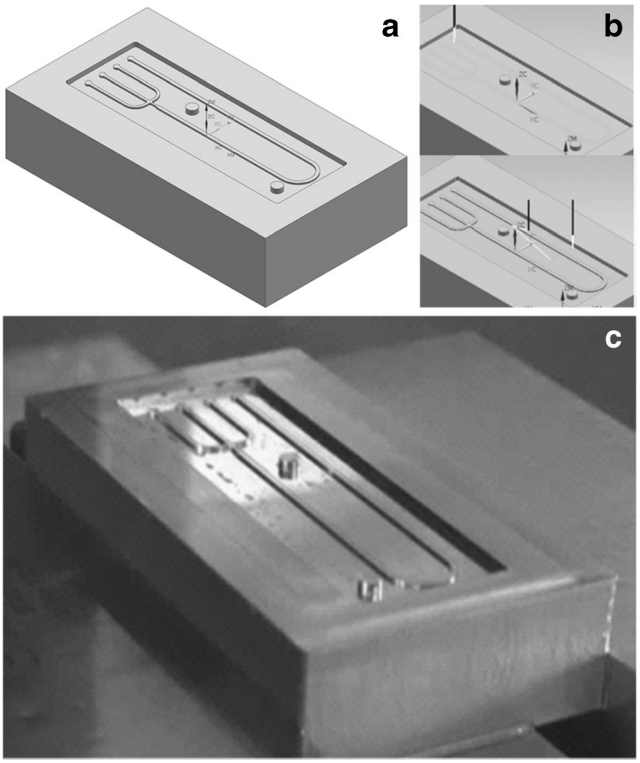

Fig. 1 Manufacturing process chain. **a** CAD design of mold with micro-features. **b** CAM tool path generation of finishing operations. **c** Machined workpiece

3 Virtual machining

The aim of micro-machining is to enable for production of miniaturized parts as well as high precision machining of functional surfaces. Micro-milling in most cases implies the application of milling tools with a diameter less than $d = 1$ mm. The cutting parameters lead to a chip thickness in the dimension of the cutting edge radius. Next, the realization of a virtual machine, tool that has been implemented within a GUI application in Matlab, Mathworks, and its applicability to simulate micro-milling processes, is roughly outlined.

3.1 The GUI application

The GUI application is divided into six modules, which are illustrated in Fig. 2: Tool Definition, Workpiece discretization,

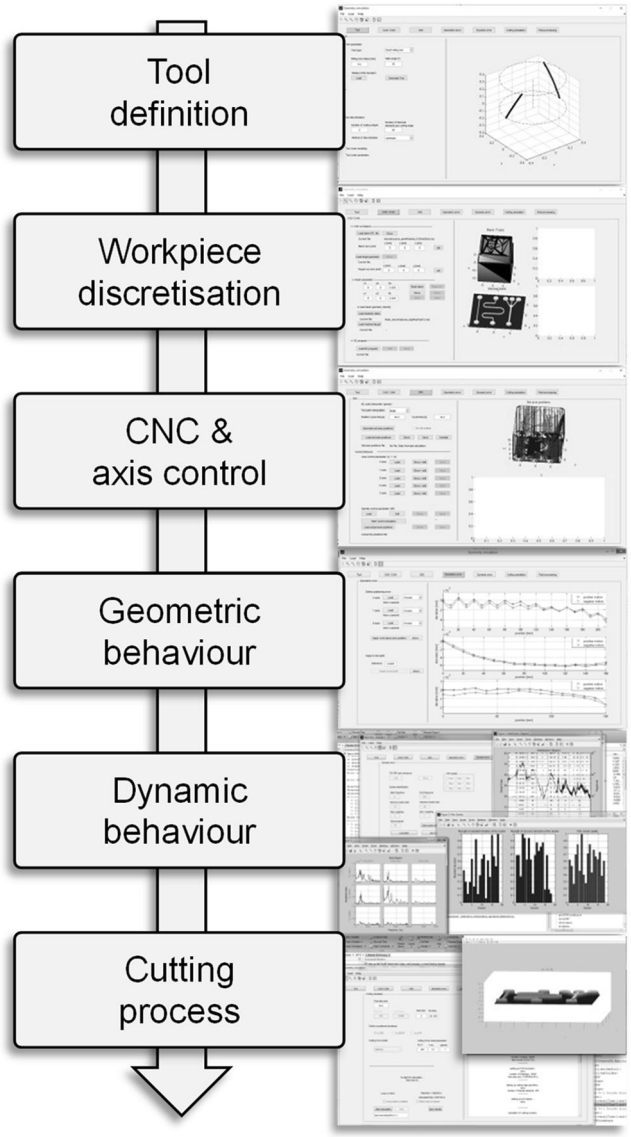

Fig. 2 Modules of virtual machine tool

CNC & axis control, Geometric behavior, Dynamic behavior, and Cutting process.

In the first module, the shaft or radius milling tool is defined and discretized. The radial position of each discretization point on the cutting edge can be set independently. This feature allows simulating any number of tool's shapes and sizes and tool wear, varying tool radius and shape within the process. In the second module, blank and target geometry can be added by a CAD file loader. The loader projects the CAD files to a parametrized user-defined mesh with coordinates X_{ij}, Y_{ij}, and Z_{ij}. Additionally, G-Code can be loaded and edited. The third module includes routines to parse and interpolate the G-Code to derive set points for a given milling process. In the fourth module, the machine geometric behavior can be regarded. A 3D geometric error model, build with results from experiments, adds position errors to the set points including backlash effects. This model gives a deviation of the TCP for each time step, which is added to the tool path generated. The dynamic behavior is implemented in the fifth module using an automatic poly-reference least-squares complex frequency (p-LSCF)-based algorithm for identification and modeling of the TCP compliance [12]. Deflections induced by calculated cutting forces are added to the set points as well during the cutting simulation. The sixth module includes simulation time control (start and end of simulation and time step size), cutting force model and parameters, and simulation file management.

3.2 Geometric cutting model

The basis for the virtual machine tool is the concept of a hitbox volume. The discretized main cutting edge is positioned relatively to the set point with added errors and deflections. To form the new surface, the points inside a triangular prism referred as the hitbox are shifted to the new position produced by the tool's cutting process. This hitbox volume is described by the movement of the cutting edges. Figure 3 shows an illustration of the proposed concept of a hitbox discretized cutting procedure. Inside the virtual machine, this concept is a simple mathematical method to isolate the mesh points affected by the cutting in each time step. To reduce even further processing time, the method considers only points within a relevant area around the TCP.

The base of this prism is a triangle formed by tree elements. The first element is a line segment between TCP and the discretized main cutting edge at a given time step T_i. The second is the same line at the next time step T_{i+1}. The last element is the line formed between the most external points of the first two elements plus an extension to account for the circular movement of the cutting edge. The prism height is the difference between the Z coordinates from the previous surface points and the TCP. The usage of this method allows geometric flexibility and independent description of cutting edges (radius, form, wear) and can be applied to radius as well as shaft milling tools.

A simple geometric test to check if the point is inside or outside of the hitbox is made for points around a relevant distance and direction of the TCP. Figure 3 also illustrates the test and shows the conditions for one point to be considered inside the hitbox. Points inside the hitbox are shifted to the new position, forming the new workpiece surface. The cutting process is conducted virtually and the resulting workpiece surface topography is calculated for each time step [13]. The position of the TCP and tool inclination is affected by geometric, kinematic, and dynamic models, in this way, forming a surface affected by the cutting parameters as well the machine behavior.

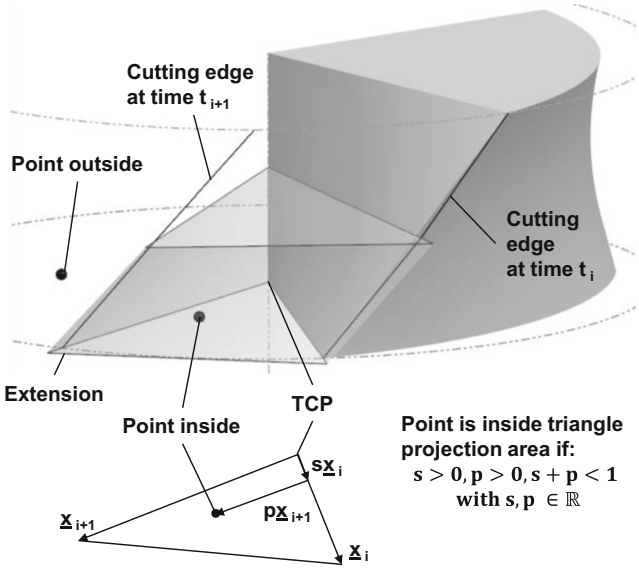

Fig. 3 Concept of a hitbox discretized cutting procedure

3.3 Cutting force model

The cutting force model is based on Kienzle equation [14], shown in Eq. (1). Additionally, a parameter describing the relation between radial and tangential cutting force is introduced and the force direction vector is described by Eq. (2). Measured cutting forces and simulation determined chip thickness, as well as radial and tangential vectors at each time step, are used to regressively determine the Kienzle parameters.

By comparing the exemplary simulated and measured cutting forces in Fig. 4, it can be observed that the virtual machine with the determined cutting force parameter yield reasonable results regarding the amplitude of F_x and F_y for micro-milling processes. Although the dynamic model has been applied and the sample rate of the simulation $f_s = 40$ kHz is comparably high, differences in f_z and high-frequency dynamic effects can be observed. One reason for this difference could come from neglecting the impact of the secondary cutting edge in the virtual machining. Stick-slip of the secondary cutting edge may be hold responsible for an excitation leading to high-frequency dynamics. This has to be investigated further.

$$F_{\text{elem}} = K \cdot K_{(WV,\text{elem})} \cdot K_{(V,\text{elem})} \cdot k_{C(i_o,h_o)} \cdot |_{\text{elem}} \cdot e_{\text{elem}} \cdot \left(h_{\text{elem}}{}^{-1-m_C}\right) \quad (1)$$

$$e_{\text{elem}} = \gamma n_r + (1-\gamma) n_t \quad (2)$$

In addition, the previous part surface was considered ideally flat in the simulations, which is not true for the real workpiece.

The Kienzle-based cutting force model required the regressive determination of specific cutting force coefficient k_c [N/mm^2], logarithmic slope parameter m_c and ratio between radial and tangential cutting force γ, each modeled with an exponential regression equation. The parameters for the material X40CrMoV5-1 were derived from preliminary tests and are shown in Eqs. (3), (4), and (5). The parameters are valid for a chip thickness range between $h = 1$ µm and $h = 1000$ µm.

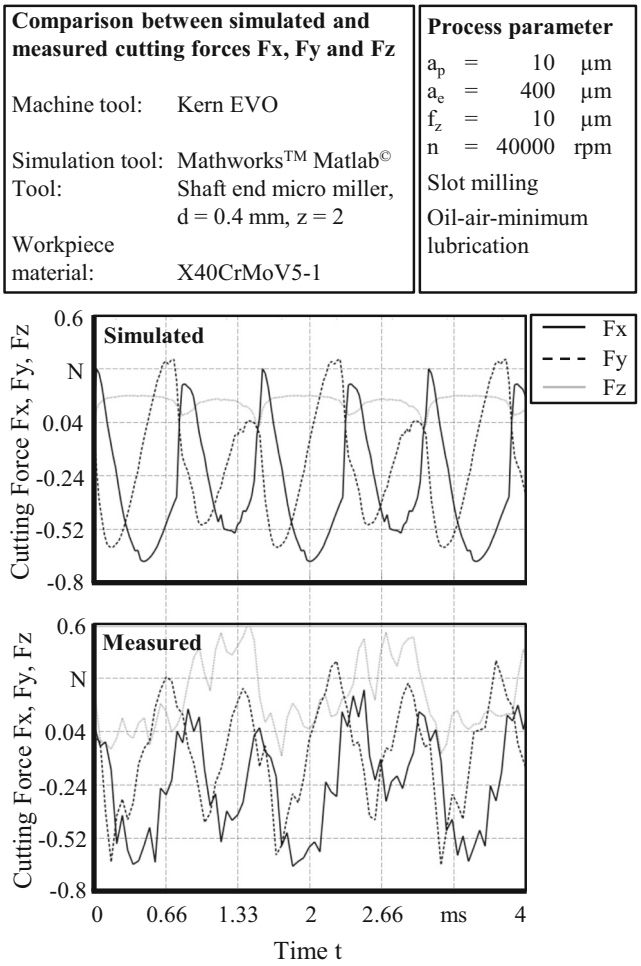

Fig. 4 Comparison of experimentally and simulation determined cutting forces

$$k_C(h) = 70e^{-300h} + 2230\left(1-e^{-10.59h}\right) \quad (3)$$

$$m_C(h) = 1-\left[0.15e^{-250h} + 0.77\left(1-e^{-48.70h}\right)\right] \quad (4)$$

$$\gamma(h) = 0.8e^{-100h} + 0.2\left(1-e^{-283.33h}\right) \quad (5)$$

The discretization impact on the accuracy of cutting force prediction has been determined for an exemplary cutting process using a tool with diameter $d = 0.4$ mm with two cutting edges, spindle speed of $n = 50{,}000$ rpm, feed per tooth of $f_z = 5$ µm, cutting depth $a_p = 30$ µm and cutting width $a_e = 0.4$ mm. It was found that convergence of mean and maximum cutting force magnitude could be reached with a mesh resolution of $d_x < 5$ µm, time step size of $d_t < 50$ µs and number of tool elements $n_t > 80$.

3.4 Tool center point dynamic rigidity

As the tools commonly used in micro-milling have small dimensions and reduced stiffness, common methods to determine the transfer functions (TF) at TCP are not suitable for these applications. Therefore, another method was applied to determine the TF. The work of Park and others describes this method [15, 16]. The KERN Evo machining center dynamic behavior has been determined in the form of TF measured at the tool chuck ESX 16. Accelerations were measured in three axis directions with an acceleration sensor type 356A12, PCB Piezo-tronics, Inc., in answer to a force excitation using a low weight self-made impulse hammer, with a force sensor measuring forces up to $F\max = 200$ N. Parallel to this process, the TF at the TCP for the system chuck and tool is determined by using the FE simulation software ANSYS 16.0, ANSYS, Inc.

Theory of model reduction offers the mathematical utilities to combine both, measurement and simulation results, and to derive a TF at the TCP considering the measurable machine tool behavior. Local maxima of the TF are between $a = 100$–350 m/s^2 on the matrix diagonal and about a dimension lower on the other matrix components. The comparison of measured and simulated TF shows difference in amplitude by almost two dimensions between simulated tool compliance and measured TF at the tool chuck. As a result, the impact of the machine tool behavior is very low in the resulting TF. The process is illustrated in Fig. 5.

To account for the TCP dynamic rigidity in the simulation tool, an automatic procedure for system identification was developed to simplify the procedure. The TCP dynamic rigidity is determined (measurement and/or simulation) in the form of full TF matrix. This matrix is inserted in the simulation tool and can be replaced to represent any machine variations. A zero-pole-gain model (ZPK) is automatically identified by applying an algorithm based on p-LSCF procedure, stability diagram information, and a related mode quality index. Cutting forces determined during machining are applied to the ZPK model and tool deflections are determined for each time step and added to the tool path.

3.5 Simulation tool results

The simulation tool generates a surface of points and a force matrix. Those results can be used to evaluate cutting conditions, machine stability, and expected surface roughness in any region of the surface. Figure 6 shows examples of the surfaces generated varying the spindle speed between $n =$ 38,000 and $n = 43{,}000$ rpm, and the force spectra for each condition. The cutting process used a tool with diameter $d =$ 0.5 mm and two cutting edges, feed per tooth $f_z = 4$ μm, cutting depth $a_p = 20$ μm and cutting width $a_e = d$. It is possible to notice the effects of an unstable cutting process on the surfaces generated with spindle speed of $n = 39{,}000$ and $n =$ 40,000 rpm, along with higher amplitudes of chatter related frequencies in the force spectra.

4 Quality inspection

The matter of inspecting miniaturized components is not trivial due to their absolute scale and feature aspect ratio. In order to evaluate the virtual machining performance, roughness on the surfaces of the mold for a micro-fluidic device, shown in Fig. 1, has been determined.

In Fig. 7, the real and the virtually machined surfaces are compared to each other. Exemplary excerpts show the height profile for the simulated and the corresponding optically enlarged machined surface. Characteristics such as milling process specific patterns and edges can be compared and show a good agreement.

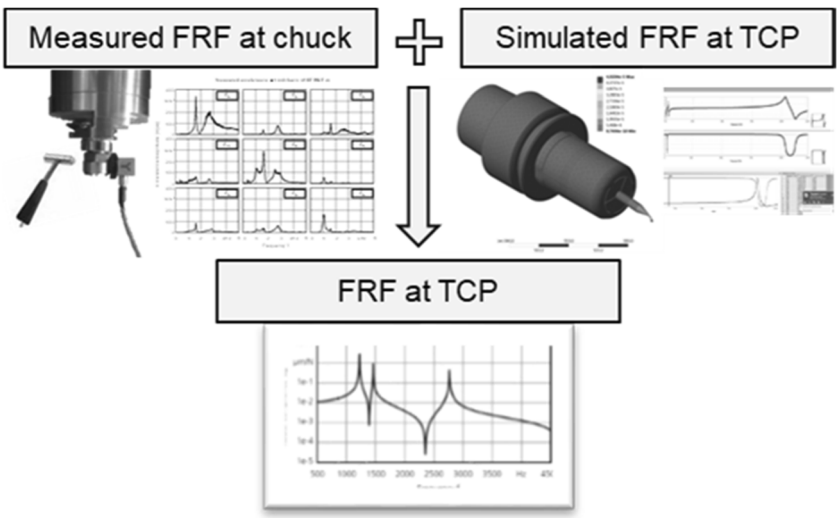

Fig. 5 Method to determine the transfer functions at tool center point

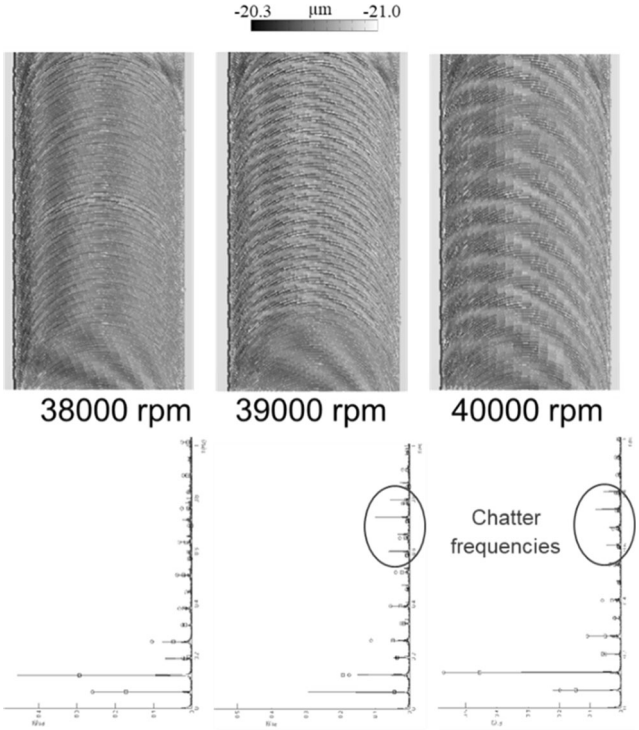

Fig. 6 Surface topographies and force spectrum for different spindle speeds

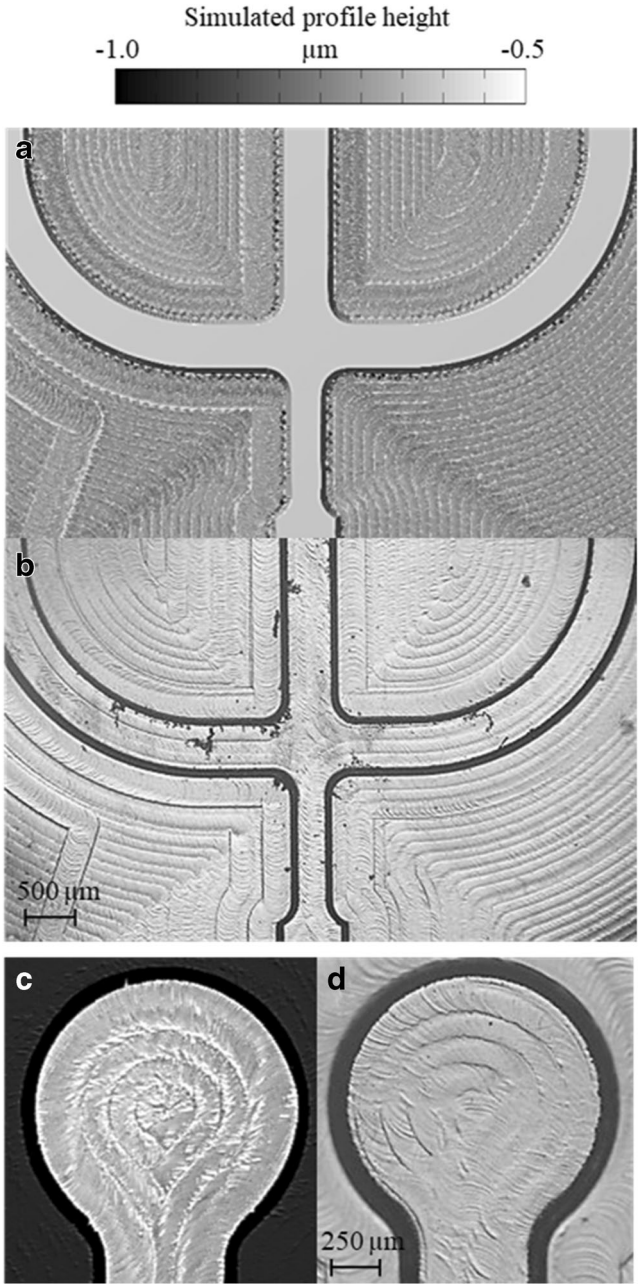

Fig. 7 Comparison of measured and simulated mold topography for simulated (**a**, **c**) and optically observed (**b**, **d**)

The roughness of the floor surface and channel top surface has been measured using a contact surface profiler Bruker Dektak XT, using line roughness parameters: center-line average roughness R_a, average peak-to-valley roughness R_z (average over five consecutive sections), peak-to-valley roughness R_t. The surface texture parameters have been selected in accordance with ISO 4288:1996 (e.g., tip radius for contact measurements and cut-off length). To separate long wavelength components from short wavelength components, the Gaussian regression filter has been applied to all roughness evaluations. Each region was evaluated in five different tracks to check within-track variation and three repetitions per track were performed to assess the pure measurement repeatability. Total measurement variation has been then calculated by ANOVA (analysis of variance) with two levels of nesting of the observations. The line roughness of the simulated surfaces has been analyzed with the same procedure that has been applied to determine roughness of the real parts' surface. The results are shown in Fig. 8.

Relative measurement uncertainties for all roughness parameters shown in the plots are below 2% of the corresponding roughness value. The roughness of the virtually machined surface is varying more than the measured roughness. Especially the surface on the top of the channels shows a significant variation which could not be confirmed to the same extent experimentally. The simulation determined and the measured line roughness values R_a, R_t, and R_z identified on the mold floor are in good agreement to each other. The peak-to-valley roughness shows a significant variation for both, floor, and channel top surface of the virtually machined mold, as it is more sensitive to profile peaks and valleys that may occur during machining. The lower roughness values for all simulation results are in the range of the measured roughness values, which may be a result of changes occurring during machining that need to be further investigated.

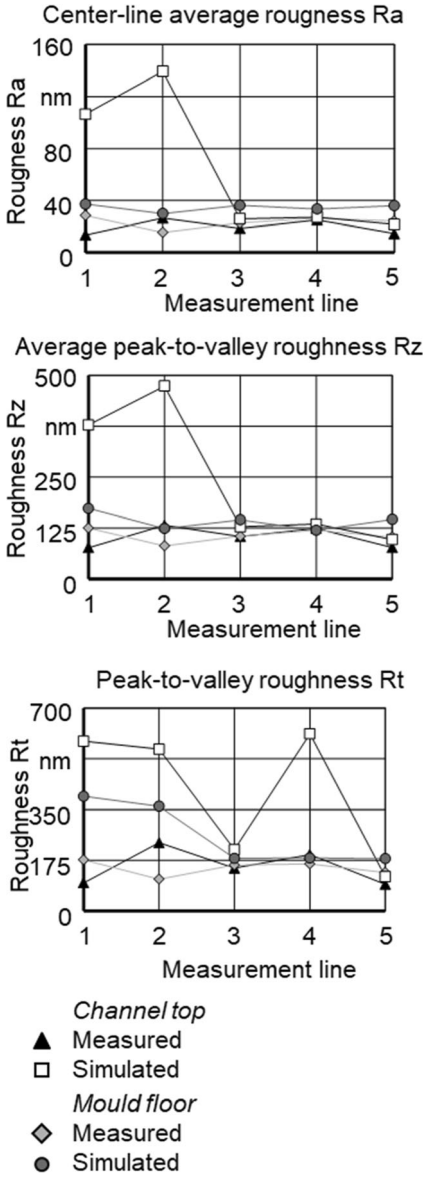

Fig. 8 Comparison of measured and simulated roughness of mold surface

5 Conclusion

The conception, development, and application of this simulation tool led to the following highlights:

- The simulation tool has a modular design and allows continuous development of additional modules and improvements to increase the similarity to the real process;
- With the tool, it is possible to easily add or remove elements that influence the cutting process and estimate its impacts, simply by changing values of the previous modules;
- This modularity also allows the creation and simulation of different scenarios to investigate and improve the real process, to find its limits, safe conditions, and optimizations. As example, the impact of changes in cutting parameters, material proprieties, or machine-tool setups and dynamic behaviors on part quality;
- The simulation also can benefit other parts of the manufacturing chain, as example, the roughness prediction can be used to highlight the critical areas for measurements supporting the metrology process.

An exemplary mold for a micro-fluidic device has been micro-milled. The mold material is the hot-work tool steel X40CrMoV5-1. The same mold has been virtually machined using a time-domain approach with discrete 2.5D workpiece and 3D tool description as well as discrete time steps. A Kienzle-based approach with chip thickness-dependent-specific cutting force, logarithmic slope and ratio between radial and tangential cutting force has been applied to determine the cutting forces. The chip thickness dependency of the cutting parameter is necessary to account for micro-scale effects. The cutting forces have been applied to a ZPK-model of the TCP compliance to derive tool deflections, which were fed back into the simulation to account for the dynamic behavior. Finally, the surface roughness of both virtually and real-machined mold has been determined as base for a comparison.

The amplitudes of simulated and measured cutting forces are in good agreement. It is difficult to distinguish between deviations that are related to issues of the force measurement process and real dynamic behavior impact. In the scope of the measurement uncertainty, it can be stated that the virtual machining model show satisfactory results. Further investigations should focus the impact of the secondary cutting edge of the shaft-milling tool on the cutting force and on the resulting surface roughness.

The roughness values determined on the surface of the virtually and real-machined mold are mostly in good agreement. Nevertheless, the simulated line roughness values show significantly higher within-region variation than the measured ones. Apparently, the virtual machining currently overestimates the roughness in some regions. For representative regions of the mold, the optical comparison of the virtual and the real surfaces is also considered. The cutting process-related patterns are indicating a good match.

Some micro-machining-related effects are somewhat arbitrary, such as the effective difference in radius of the two cutting edges, which can vary for different tools or the form of the minor cutting edge. Furthermore, the identification of the cutting edge radius dependency of minimum chip thickness and ratio between radial and tangential cutting force would demand for a very precise determination of the tool geometry. Further investigations should emphasize the probability of different tool conditions and their impact on the machining process.

References

1. Ardila LKR, Ramos LWSL, Del Conte EG, Abackerli AJ, Picarelli TC, Perroni FAO, Schützer K, Mewis J, Uhlmann E (2015) Micromilling process for manufacturing of microfluidic moulds, 23rd ABCM ICME. Proceedings of the 23rd ABCM International Congress of Mechanical Engineering, Rio de Janeiro, Brazil
2. Tosello G, Hansen NH, Gasparin S (2009) Applications of dimensional micro metrology to the product and process quality control in manufacturing of precision polymer micro components. Ann CIRP Manuf Technol 58:467–472
3. Petz M, Tutsch R, Christoph R, Andraes M, Hopp B (2012) Tactile–optical probes for three-dimensional microparts. Measurement 45:2288–2298
4. Hansen HN, da Costa Carneiro K, Haitjema H, De Chiffre L (2006) Dimensional micro and nano metrology. Ann CIRP 55(2):721–743
5. Fleischer J, Lanza G, Schlipf M (2008) Statistical quality control in micro-manufacturing through multivariate μ-EWMA chart. Ann CIRP Manuf Technol 57(1):521–524
6. Uhlmann E, Schauer K (2005) Dynamic load and strain analysis for the optimization of micro end mills. Ann CIRP 54(1):75–79
7. Altintas Y, Jin X (2011) Mechanics of micro-milling with round edge tools. Ann CIRP Manuf Technol 60(1):77–80
8. Biermann D, Krebs E, Sacharow A, Kersting P (2012) Using NC-path deformation for compensating tool deflections in micromilling of hardened steel, 5th CIRP conference on high performance cutting. Procedia CIRP 1:132–137
9. Uhlmann E, Mahr F (2012) A time domain simulation approach for micro milling processes. 3rd CIRP conference on process machine interactions. Procedia CIRP 4:22–28
10. Mamedov A, Layegh SE, Lazoglu I (2013) Machining forces and tool deflections in micro milling, 14th CIRP CMMO. Procedia CIRP 8:147–151
11. Altintas Y (2016) Virtual high performance machining, 7th CIRP conference on high performance cutting. Procedia CIRP 46:372–378
12. Uhlmann E, Kushwaha S, Mewis J, Richarz S (2017) Automatic design and synthesis of control for a plug and play active vibration control module. J Vib Control
13. Uhlmann E, Abackerli AJ, Schützer K, Lepikson HA, Helleno AL, Papa MCO, del Conte EG, Mewis J (2014) Simulation and analysis of error impact on freeform surface milling. Int J Adv Manuf Technol 70(1–4):607–620
14. Kienzle O, Victor H (1952) Die bestimmung von kräften und leistungen an spanenden werkzeugmaschinen. VDI-Z 94:299–305
15. Park SS, Altintas Y, Movahhedy M (2003) Receptance coupling for end mills. Int J Mach Tools Manuf 43:889–896
16. Mascardelli B, Park SS, Freiheit T (2008) Substructure coupling of micro end mills to aid in the suppression of chatter. ASME J Manuf Sci Eng 130